A latitudinal network of GPS receivers dedicated to studies of equatorial spread *F*

C. E. Valladares and R. Sheehan

Newton Resource Center, Institute for Scientific Research, Boston College, Chestnut Hill, Massachusetts, USA

J. Villalobos

Department of Physics, Universidad Nacional de Colombia, Bogota, Colombia

Received 5 December 2002; revised 15 March 2003; accepted 27 May 2003; published 12 February 2004.

[1] Five GPS receivers have been deployed near the 74°W longitude meridian to measure the variability of total electron content (TEC) latitudinal profiles and to study the relation of this variability with the onset and evolution of spread *F* plasma structures. These five GPS receivers, together with two others that form part of the International GPS Service (IGS) network, three more that belong to the South Andes Project network, and an additional receiver located at Ancon, Peru, provide TEC values between 8°N and 40°S geographic latitude. In addition, all five GPS receivers managed by Boston College give the amplitude scintillation on a near-real time basis. This fact allows us to know the maximum latitude to which the irregularities extend and to infer the maximum altitude of the plasma bubbles. We have calculated TEC latitudinal profiles using the TEC values obtained by all the receivers between 1998 and 2001. We found that during the equinoxes, UHF scintillations occur when the ratio of the crest to the trough of the anomaly is 2 or larger. During the December solstice the crest is not very pronounced, but a sharp decrease of TEC at the magnetic equator precedes the onset of 1-km scale irregularities. We have also examined a longitudinal variability of scintillations by partitioning the sky in two sectors separated at the 74°W meridian. We consistently observe a greater number of GPS scintillation events at the eastern longitudes over the Amazon rain forest. This intriguing finding could well be explained by a larger population of gravity waves at longitudes east of the Andes. *INDEX TERMS:* 2415 Ionosphere: Equatorial ionosphere; 2439 Ionosphere: Ionospheric irregularities; 2471 Ionosphere: Plasma waves and instabilities; *KEYWORDS:* equatorial spread *F*, scintillations, equatorial anomaly, gravity waves, plasma bubbles

Citation: Valladares, C. E., R. Sheehan, and J. Villalobos (2004), A latitudinal network of GPS receivers dedicated to studies of equatorial spread *F*, *Radio Sci.*, *39*, RS1S23, doi:10.1029/2002RS002853, in press.

1. Introduction

[2] The equatorial spread *F* (ESF) phenomenon consists of the sudden advection of a region 100 to 500 km wide containing low-density plasma [*Woodman and LaHoz*, 1976]. This unstable plasma originates at the bottomside of the *F* region and rises, in most cases, up to the topside of the *F* layer. While ESF was initially used to describe plasma bubbles and the irregularities that grow within them, it is used now to denote other types of structures seen at low latitudes such as bottomside sinusoids (BSS) [*Valladares et al.*, 1983] and bottomside and bottomtype traces [*Hysell and Burcham*, 1998].

[3] When a radio wave propagates through a medium containing plasma structures (equatorial spread *F*), the signal suffers amplitude and phase distortions. If the level of the structuring is low, only the phase and the angle of arrival are changed (thin phase screen). If the structuring level is strong, the amplitude of the signal also varies (thick phase screen). After crossing the phase screen, the electromagnetic wave is affected by strong interference, and a diffraction pattern in both intensity and phase develops at the ground. These fluctuations of the radio signals are known as scintillations; they are more common in the VHF, UHF, and L-band frequency range. Weak and strong levels of scintillations can

0048-6604/04/2002RS002853$11.00

produce disruptions of the communication and navigation links that use low- or high-altitude orbiting satellites. Fadeouts of GPS signals cause, in some cases, an additional error in the location of the site, which could be as large as tens of meters. In other cases, a complete loss of the navigation capability may occur. The disruption of communication signals and the degradation of navigation capabilities constitute the main incentive to develop a forecasting capability of the onset of irregularities and to closely monitor the evolution of the spread *F* phenomenon.

[4] In the last two years, Boston College has installed five GPS receivers at different locations in Colombia and Peru. Two receivers were installed in Bogota and one in each of the cities of Iquitos, Pucallpa, and Cuzco. These new receivers are providing values of the S4 scintillation index, and together with the IGS and SAP GPS receivers, they give the latitudinal distribution of TEC. This paper presents the statistics of the latitude extension of GPS scintillations as seen by some of the GPS receivers operating near and north of the magnetic equator and the characteristics of the TEC latitudinal profiles as a function of ESF activity. The onset of ESF was determined on the basis of the appearance of UHF scintillations measured at Ancon near the magnetic equator. For a single case study we also compare the maximum latitude of scintillations to the altitude extension of radar plumes recorded with the JULIA radar.

2. TEC Latitudinal Profiles

[5] Figure 1 shows the location and the TEC field-of-view of the GPS receivers that belong to the IGS, the North Andes Project (NAP), and the South Andes Project (SAP) networks. At present the IGS stations (Arequipa and Santiago) and the SAP receivers (Iquique, Copiapo, and Antuco) produce data files that are made available to us on an off-line basis. The Boston College (BC) receivers measure the S4 index using the L1 frequency. Their scintillation field-of-view covers a latitudinal region extending between 21°S and 11°N geographic latitude (−9° and +23° magnetic latitude). An additional receiver, to be located at the northern boundary of Colombia, should allow us to detect the exceptional events when scintillations reach 15°N latitude (∼27° magnetic latitude) or plasma bubbles extending up to 2000 km. Figure 1 also displays the ground projection of a field line that passes above the Jicamarca station reaching an apex altitude of 1610 km.

[6] Figures 2, 3, and 4 display the result of subtracting the TEC distribution measured at 1800 LT and the values at 2000 LT. In mathematical form, this is expressed as

$$d\mathrm{TEC} = \mathrm{TEC}(1800) - \mathrm{TEC}(2000).$$

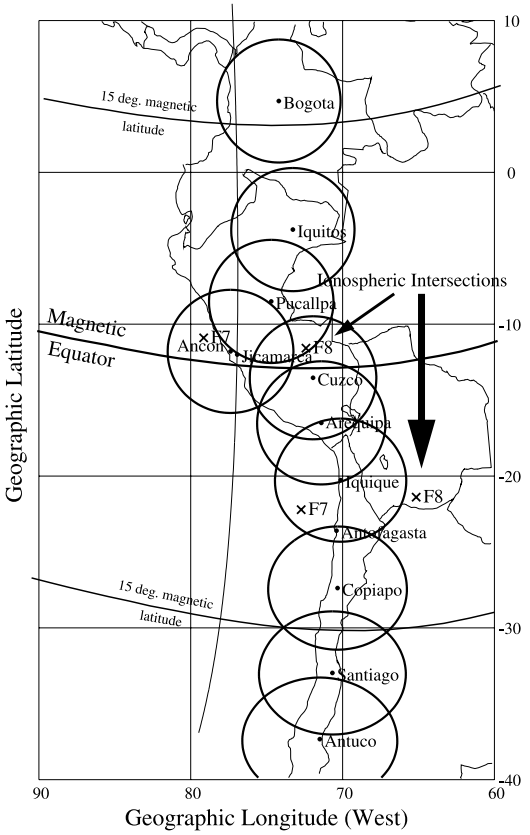

Figure 1. Geographic locations and field-of-views of several GPS receivers operating near the west coast of South America. The stations at Ancon, Cuzco, Pucallpa, Iquitos, and Bogota form the North Andes Project (NAP) network. The stations of Iquique, Copiapo, and Antuco form the South Andes Project (SAP), and the stations of Arequipa and Santiago form part of the IGS network of receivers. The fields-of-view encircling the stations are for 35° elevation angle and an altitude of 350 km. The near-vertical line that crosses the Jicamarca station corresponds to the ground projection of a field line with a 1610 km apex altitude and feet at 350 km altitude.

Positive values of *d*TEC indicate a temporal reduction of the TEC distributions; negative *d*TEC values indicate a temporal growth in TEC. Figure 2 shows *d*TEC values for all nights in 1999 when UHF scintillations are seen at both Ancon and Antofagasta stations. These curves show a strong latitudinal variability during all 8 months of scintillation activity. The *d*TEC values at latitudes near the magnetic equator (∼12°S geographic latitude) are 30 units or larger. On a few days during the months of March, October, and November, the TEC value at the magnetic equator reaches 50 units. At latitudes corresponding to the peaks of the anomaly (near 4°N and 28°S), the *d*TEC values are near zero and are in many

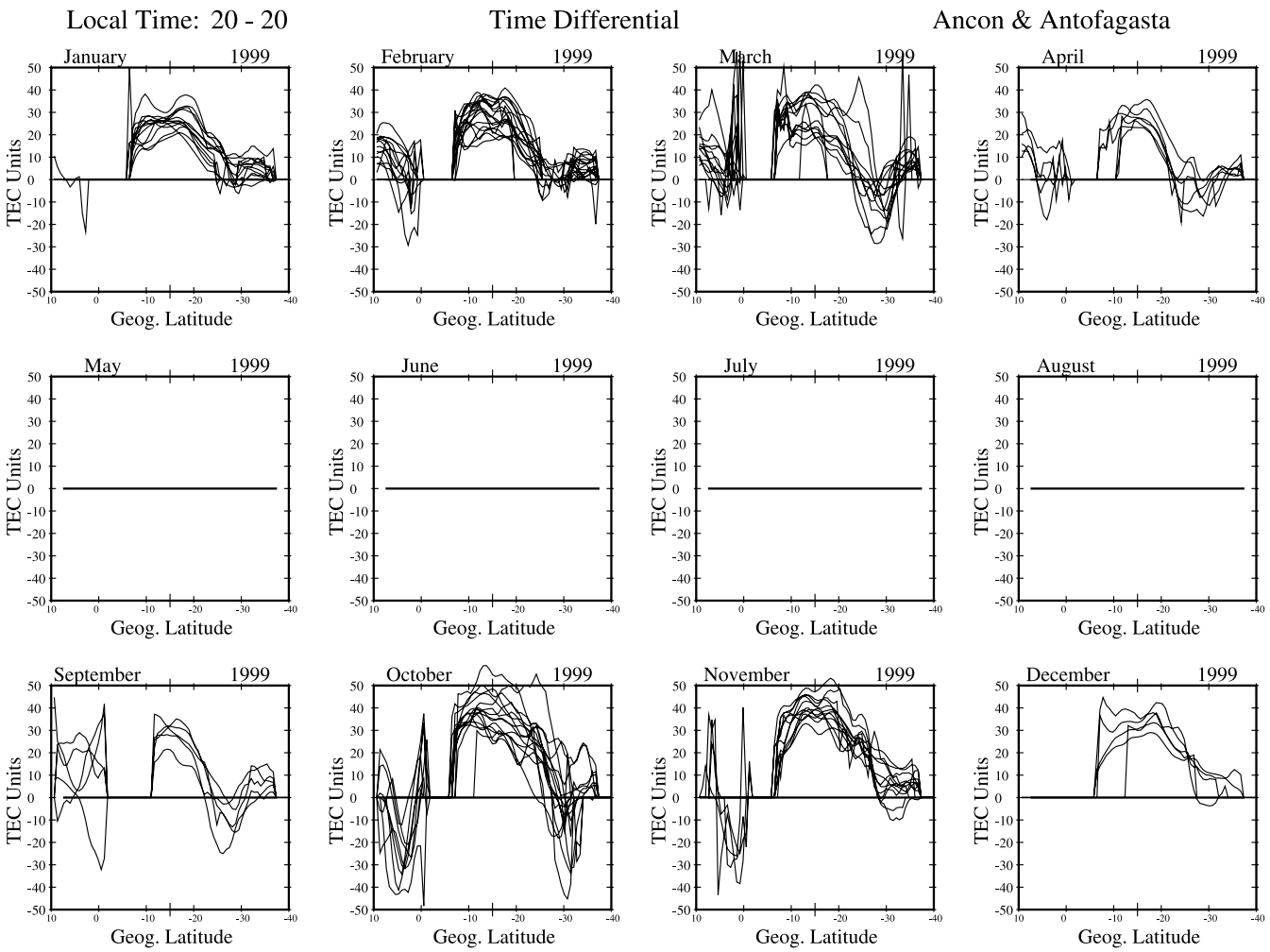

Figure 2. TEC latitudinal distribution of the difference of the curves corresponding to 1800 LT and the traces for 2000 LT. Only days when scintillations occurred at Ancon and Antofagasta are considered here.

cases negative. This variable pattern indicates that between 1800 and 2000 LT, the TEC value of the crests increase and the trough diminishes during days when ESF occurs. This behavior reflects the changes in the *F* region that occur right after sunset. *Fejer et al.* [1999] introduced Jicamarca measurements that provided evidence for the appearance of a fully developed prereversal enhancement (PRE) of the vertical drift during nights of ESF activity. In agreement with this idea, *Valladares et al.* [2001] presented TEC latitudinal profiles obtained in 1998 indicating that the PRE is able to reenergize the equatorial fountain effect, deplete the density near the equator, and simultaneously increase the density near the crests of the anomaly. This plasma dynamics explains the general characteristics of the *d*TEC curves. However, the profiles corresponding to 1999 and 2001 (Figure 3) show an additional effect that was not seen in the latitudinal profiles of 1998 [*Valladares et al.*, 2001]. During the months of January, February, November, and December, the negative *d*TEC values are seen only in the northern crest, while the southern crest shows values near zero. This is more evident in the frame corresponding to November 2001 (Figure 3), where *d*TEC values are near −50 TEC units at the location of the northern crest but near zero at latitudes typical of the southern crest. Figure 4 shows the *d*TEC profiles for days when no scintillations were seen at the Ancon and the Antofagasta sites. In this figure, all the curves are more uniform, displaying values less than 30 TEC units near the magnetic equator. At crest latitudes the *d*TEC values are in most cases near 20 units. Only two cases, one in October 1999 and the other in November 1999, show significant negative (less than −10 TEC units) *d*TEC values near the northern crest.

[7] Figure 5 displays a statistical distribution of the crest TEC value as a function of the trough TEC value for years 1999, 2000, and 2001. The red dots correspond

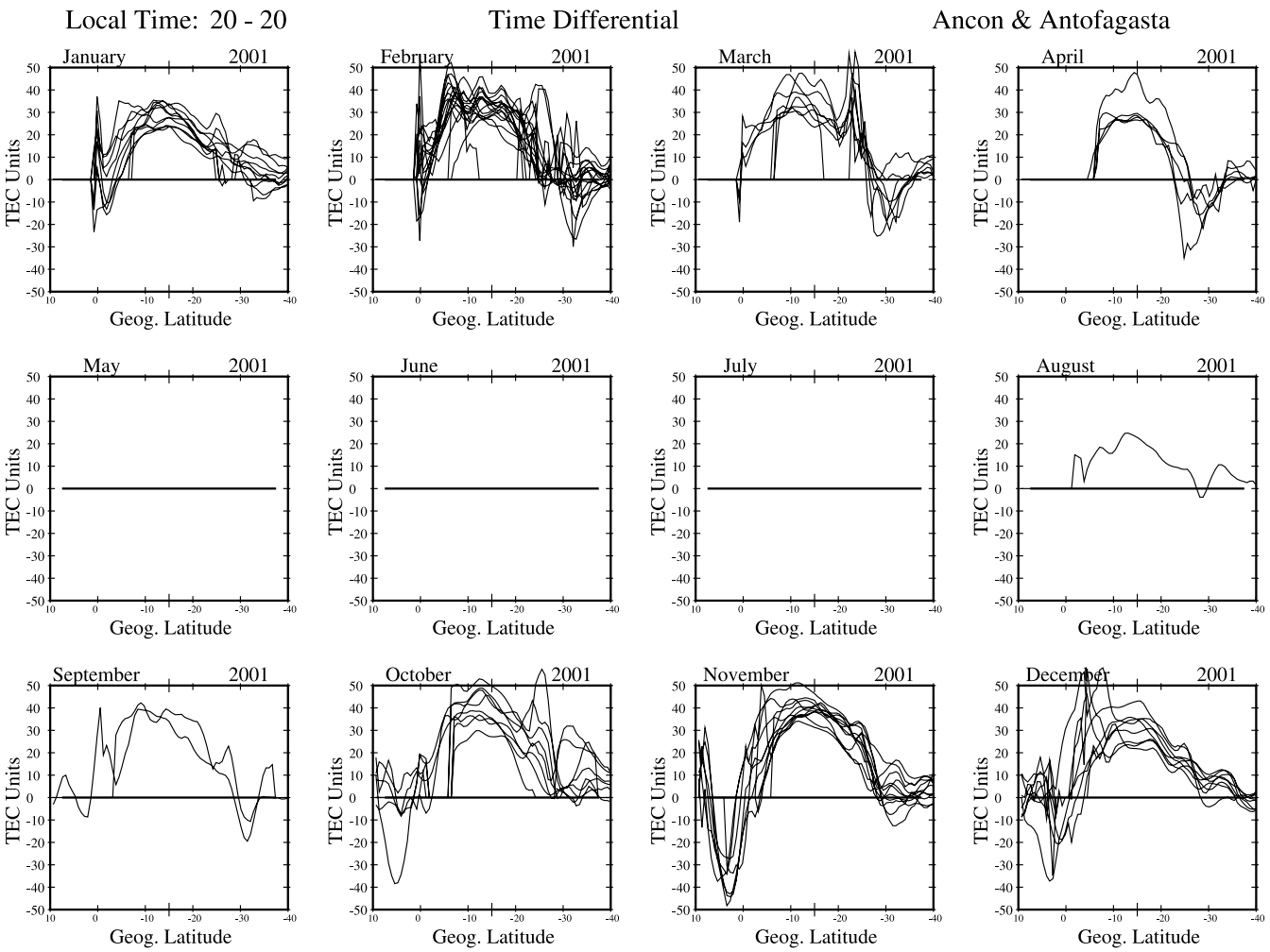

Figure 3. Same as Figure 2 but for year 2001.

to events when scintillations are present and the blue dots to times of no scintillation activity. The scintillation events are mainly restricted to small trough TEC values and large amplitude of the crests. The no-scintillation cases consist of large trough values and are placed in regions to the right but adjacent to the red dots. This figure also indicates that the peak value of the crests is the largest during the equinoctial months (March, April, October, and November). It is between 40 and 120 units during the months of January, February, September, and December and the smallest during the June solstice (May, June, July, and August). Figure 6 shows a mass plot of the peak-to-trough ratio as a function of local time for all the TEC latitudinal profiles that were obtained in 1999 during the nighttime hours (1900–0700 LT). The left panel exhibits the ratios for events of premidnight scintillations; the right panel displays all cases of no scintillations. Large color-coded dots are used to indicate the average value for every 1-hour bin. The scintillation events exhibit ratios above 1.5 and present a large dispersion with most of the values larger than 2. The no-scintillation events have ratios less than 1.5, small spread, and 1-hour averages near 1.3. This prominent difference in the characteristics of the TEC profiles, which are highly dependent on the scintillation activity, points to an inherently different behavior of the drivers of the equatorial *F* region dynamics during nights when scintillations occur.

3. GPS Scintillation Latitudinal Profiles

[8] The top panels of Figure 7 show the scintillation S4 index measured by the Bogota, Iquitos, and Cuzco stations between 19 and 23 LT on 5 September 2002. The lower panel exhibits the coherent echoes measured by the JULIA radar during the same day. A single plume is observed at 2040 LT, extending up to 1610 km altitude. However, the westward tilt of the plume makes the topside part of the coherent echoes to be detected by JULIA near 2115 LT. GPS scintillations were observed

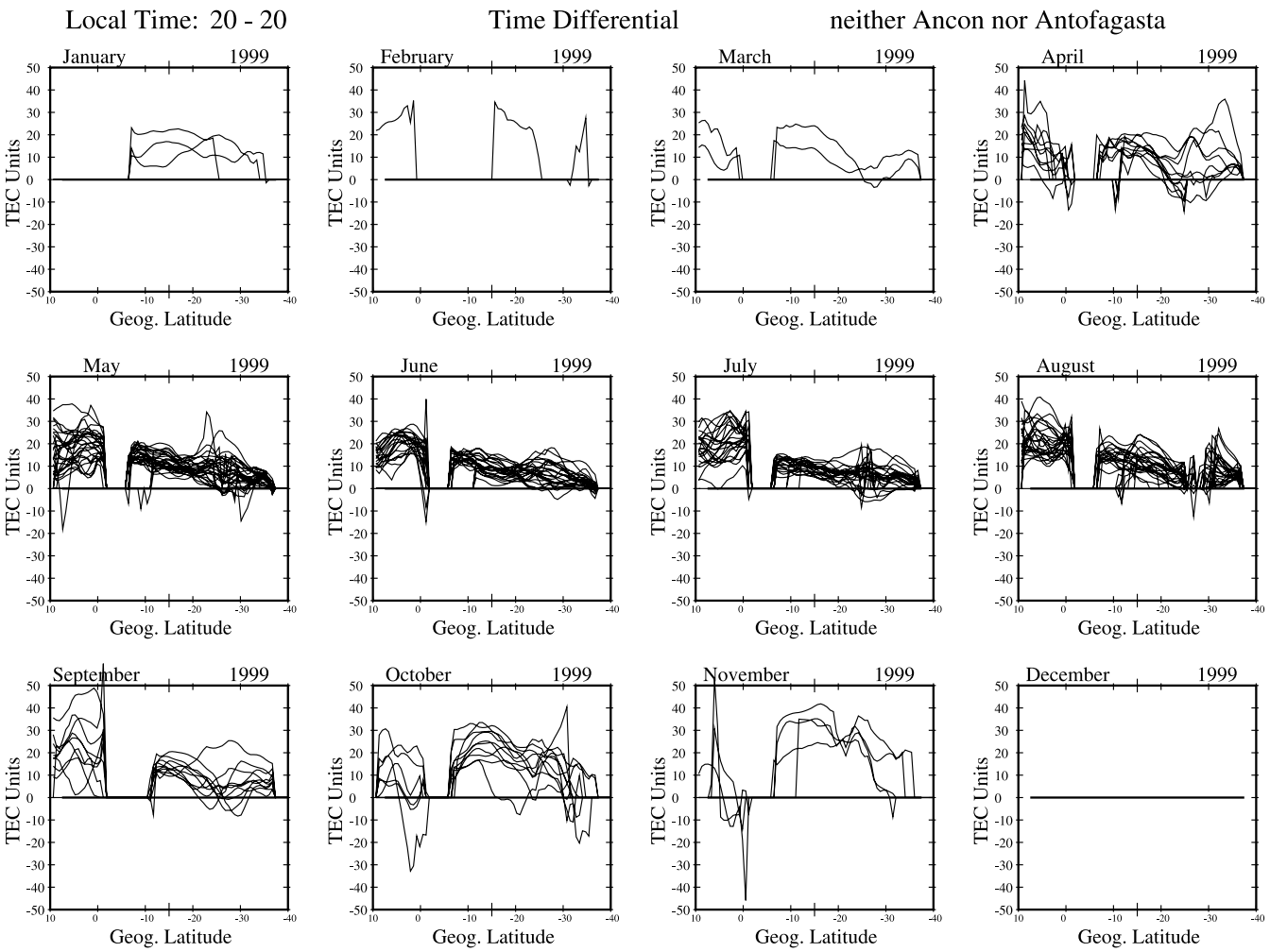

Figure 4. Same as Figure 2 but for days of no scintillations at both stations.

from Bogota reaching 11°N latitude (∼23°N magnetic latitude) at the 78°W meridian between 2050 and 2130 LT (see arrow). As indicated in Figure 1, the field line over Jicamarca with an apex altitude of 1610 km intersects the *F* region at 11°N latitude. Consequently, the location and the local time of the GPS scintillations are in very good agreement with the observations of a plume reaching 1610 km altitude that was observed with the JULIA radar.

[9] On the basis of the excellent agreement that exists between the altitude of the plasma plumes observed with the JULIA radar and the maximum latitude of the scintillation S4 index measured with the GPS L1 band, we decided to use the maximum latitude of the GPS scintillation as a proxy for the altitude of the plasma plumes. Figure 8 shows the magnetic latitude distribution of the scintillations detected by the systems located at Bogota, Iquitos, and Cuzco between 28 August 2001 and 28 February 2002. We have used arrows that point to a small segment to indicate the maximum latitude at which scintillations were observed during each individual day. We also divided the field of views of the three stations in two sectors. One sector, labeled west, included all the S4 values detected to the west of the 74°W meridian. The east observations indicated the scintillations seen to the east of the 74°W meridian. It is evident that more scintillation events exist on the east side, and for a larger number of cases the maximum latitude reached values up to 23° magnetic latitude (∼11°N geographic latitude). It is important to mention that Bogota is located close to the 74°W meridian, and almost the same number of GPS satellites is seen to the west and east of each meridian. It is also evident that during several nights the maximum latitude (and the altitude of the plumes) exceeded the northern boundary of the field-of-view of the Bogota station that is limited at 12°N latitude.

[10] Figure 9 shows histograms of the number of days when scintillations reached the maximum magnetic latitude indicated on the horizontal axis. The histogram on the left side includes all the observations between

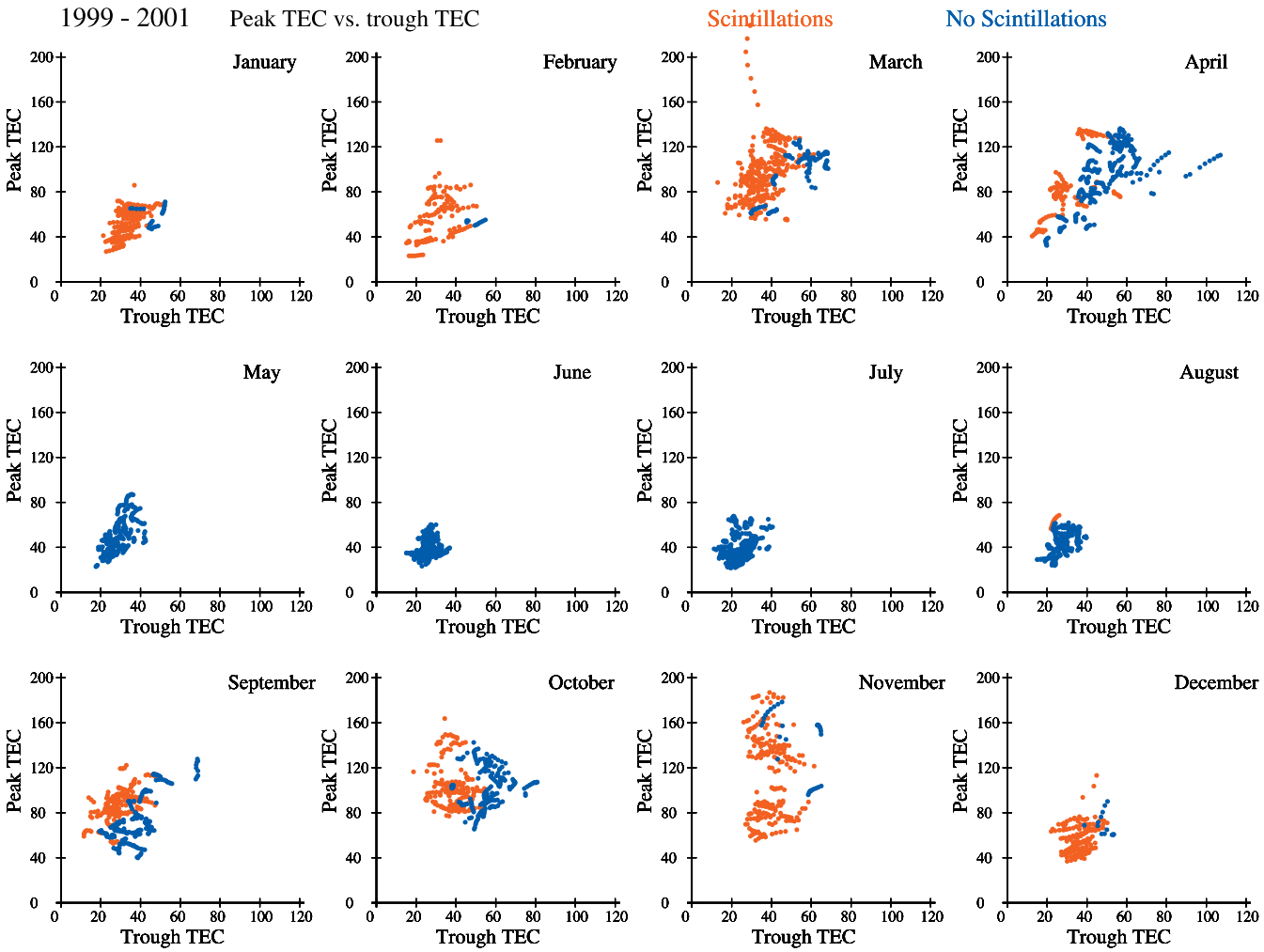

Figure 5. Monthly mass plots of the crest TEC value as a function of the trough TEC value extracted from the latitudinal profiles for years 1999–2001. The red dots are coded for days of scintillations and the blue dots for days of no scintillations.

28 August 2001 and 28 February 2002. The histograms at the center and the right side correspond to the west and east sectors as defined above. Figure 9 explicitly indicates that more events are seen in the east sector than in the west side. In addition, the average maximum latitude is larger to the east than to the west. While prominent difference in scintillation activity have been seen by stations separated by few hundred kilometers [*Basu et al.*, 2001] during magnetically disturbed days, we did not expect to find that statistics of 180 days, most of them during quiet magnetic conditions, would give such different results.

4. Discussion

[11] Figure 2 indicates that during the equinoctial and December solstice months the fountain effect, which is driven by the upward vertical drift, is in effect when scintillations are simultaneously observed at both Ancon and Antofagasta. This evidence endorses the role of the vertical drift velocity as the controlling parameter in the generation of spread *F* irregularities [*Fejer et al.*, 1999]. These authors associated the occurrence of a large PRE with the initiation of equatorial spread *F*. We suggest that the same upward drift, which drives the *F* region to higher altitudes, creates a postsunset resurgence of the fountain effect. Thus Figures 2 and 3 are indirect proof of the control that the equatorial electrodynamics, and specifically the upward vertical drift velocity, exerts on establishing the right conditions for the development of ESF. This result agrees with data recently presented by *Valladares et al.* [2001]. This latter study presented latitudinal distributions of TEC obtained in 1998 to demonstrate that the temporal difference of TEC showed

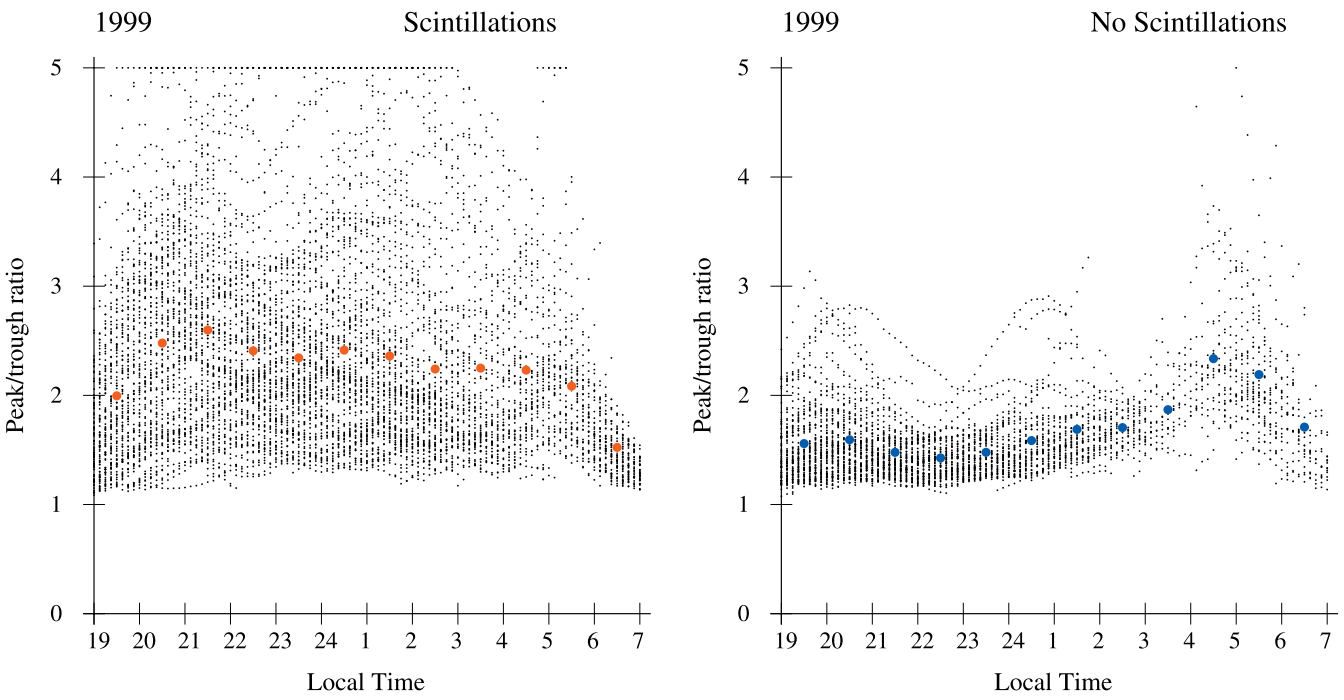

Figure 6. Scatterplot of the peak-to-trough ratio versus local time for all the TEC distributions in which scintillations were observed in 1999. The average value (large red dots) is above 2 between 2000 and 0600 LT. The right panel corresponds to nights of no scintillations. In this frame the average values (blue dots) are near 1.5 between 1900 and 0300 LT.

quite drastic increases of the crest values and sharp decreases near the trough during days when strong scintillations were observed. In addition, Figures 2 and 3 showed that during the solstice months (November through February) the *d*TEC distributions were clearly asymmetric. A large negative value of order 50 TEC units was seen near latitudes typical of the northern crest and small values ($\sim$0) around the southern crest. This fact indicates that between 1800 and 2000 LT the TEC profile developed into a highly asymmetric distribution with a prominent northern crest and a much smaller southern peak. This effect is probably caused by a strong northward directed meridional neutral wind. The appearance of asymmetrical distributions, mainly during the December solstice months, agrees well with the season of larger meridional winds and times when the low-latitude thermospheric wind blows toward the north.

[12] *Maruyama and Matura* [1984] suggested that the meridional wind was able to suppress the growth of the Rayleigh-Taylor instability (RTI) and hence to control the ESF activity. The numerical calculations of *Maruyama* [1988] indicated that the transequatorial wind was able to depress the *F* layer in the lee-side hemisphere and consequently change the field-integrated Pedersen conductivity [*Mendillo et al.*, 1992]. This evidence suggested that a southward wind was somewhat responsible for lowering the density contours and for making the whole flux tube more stable to the onset of the RTI. More recently, *Mendillo et al.* [2001] used measurements from a Fabry-Perot Interferometer (FPI) and an imager to conclude that during 8 days of a campaign in September 1998 the meridional wind did not influence the onset of ESF in the premidnight hours. Our finding reinforces this idea and indicates that for years of high solar activity the meridional wind may not be able to inhibit the growth of ESF irregularities. *Devasia et al.* [2002] have presented evidence suggesting that when $h'F$ is below 300 km, ESF may occur only for a thermospheric meridional wind directed equatorward and less than 60 m/s. The *d*TEC curves shown by *Valladares et al.* [2001] for a year of low solar activity did not display the asymmetry that was presented in the data corresponding to 1999 and 2001. Therefore the more symmetric curves of 1998 may confirm the need for the meridional wind to be small during years of low solar flux and to be unimportant during years of high solar activity.

[13] The consistent difference in scintillation activity between two adjacent longitudinal sectors suggests the presence of a suppressor (or intensifier) mechanism on the west (east) side of the 74°W meridian. Penetrating electric fields of magnetospheric origin have been suggested to be localized in longitude [*Basu et al.*, 2001] and do produce

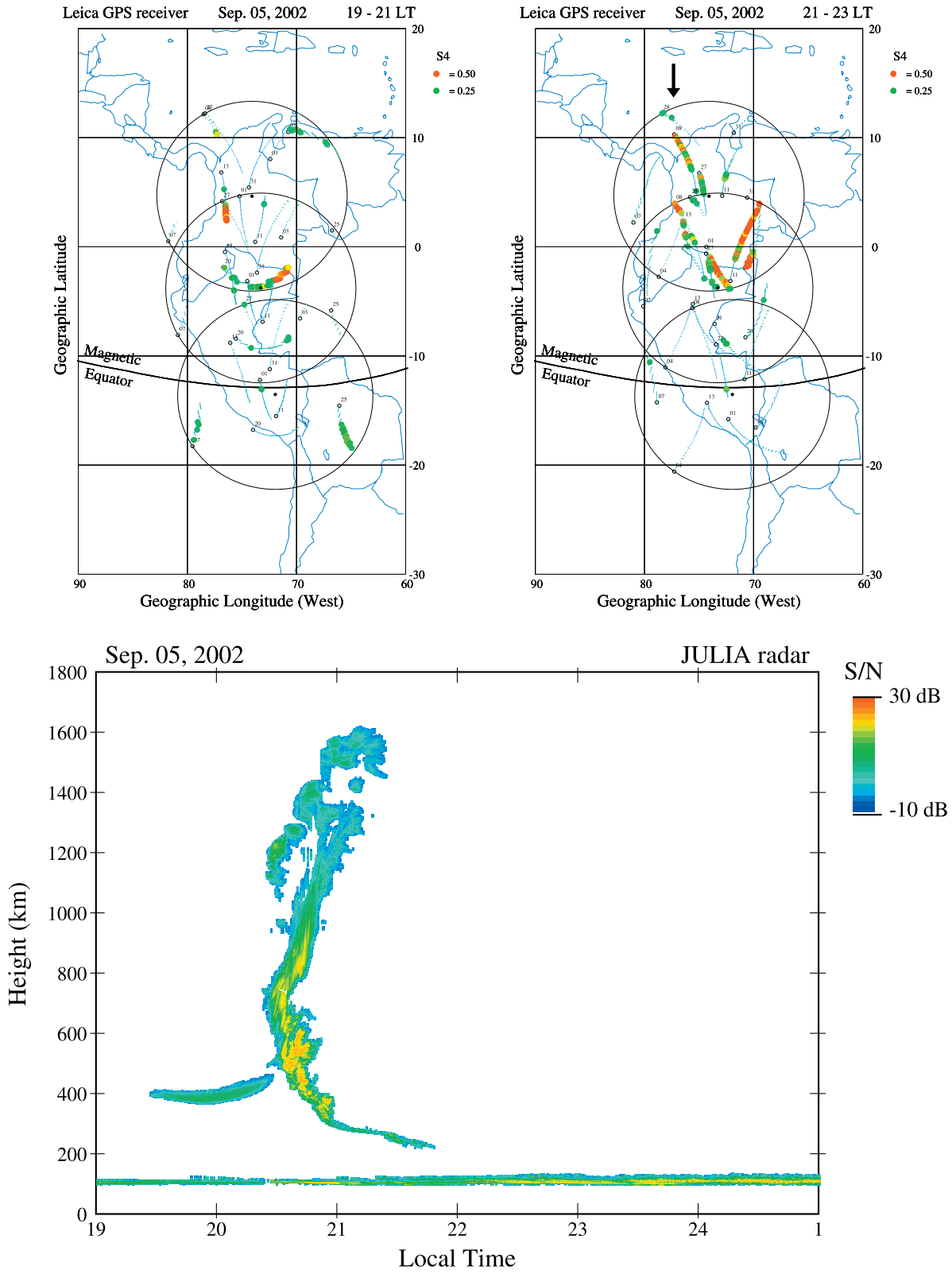

Figure 7. Top panels show the scintillation S4 index measured by the GPS receivers installed at Bogota, Iquitos, and Cuzco during two 2-hour periods. The lower panel displays a power map of coherent echoes detected by the Julia radar. Note that scintillations are seen up to 11°N latitude at the same time and location when the JULIA radar observed a plume extending up to 1610 km altitude.

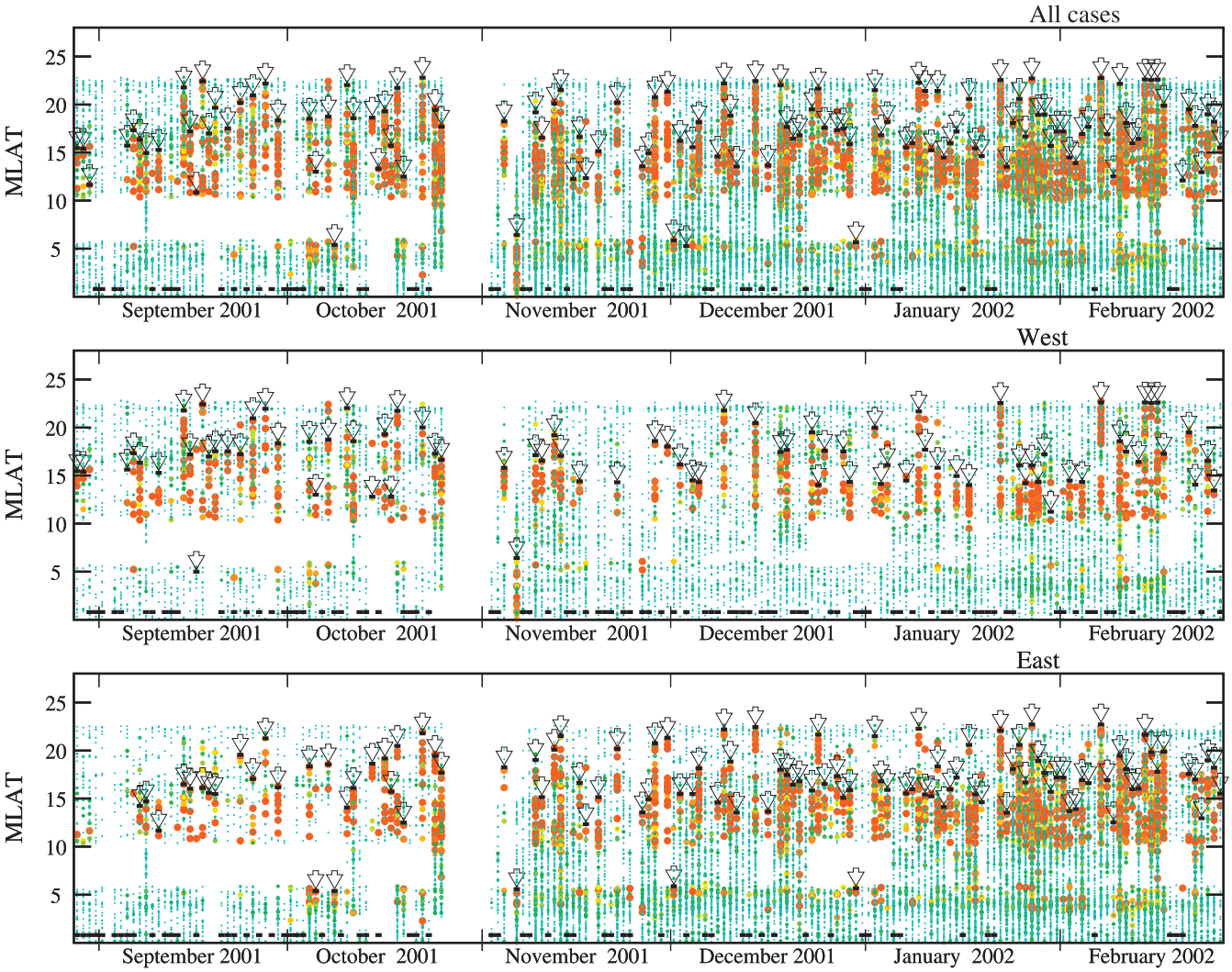

Figure 8. Map of scintillation activity for days between 28 August 2001 and 27 February 2002. The magnitude of the S4 index has been color-coded with red meaning values larger than 0.5, the green dots equal to 0.25, and the small blue dots indicate recording noise level. The vertical axis is the magnetic latitude at which the scintillations were observed. The arrows point to the latitude of the third polewardmost point of S4 values above the noise level (0.20).

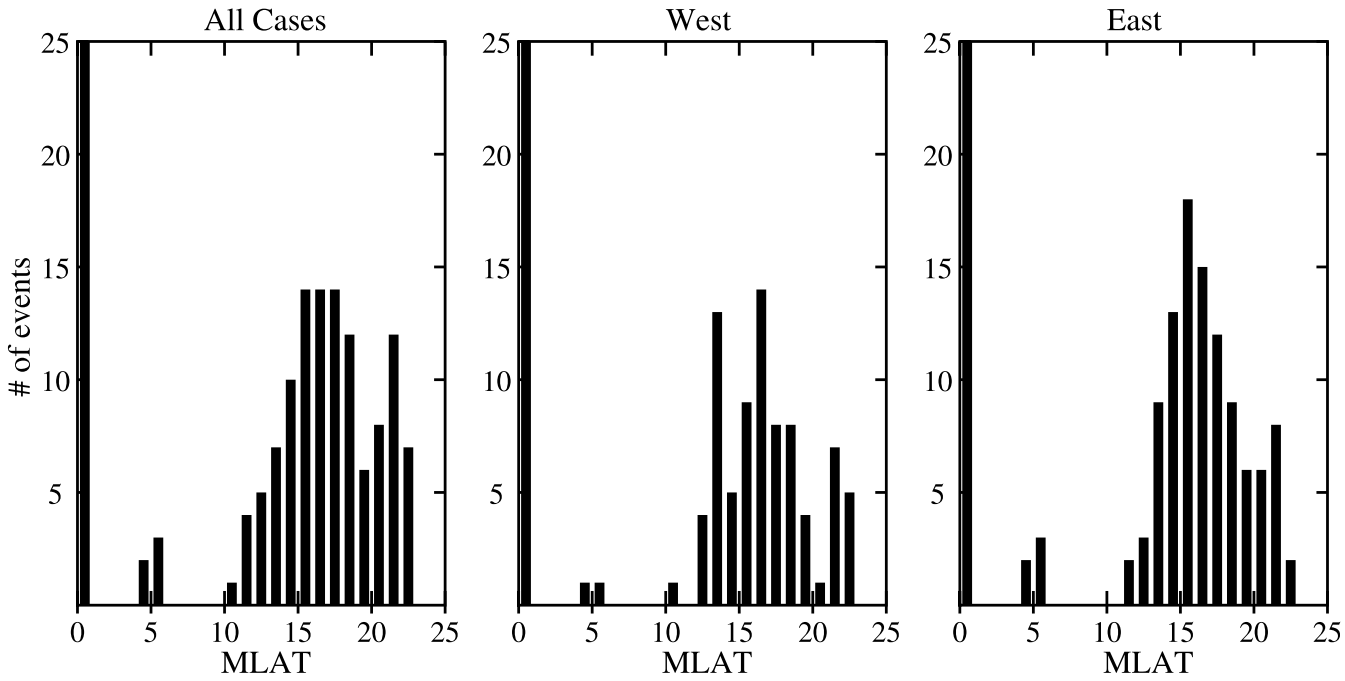

Figure 9. Statistical distribution of the number of days and the maximum latitude where scintillations (S4 > 0.20) were observed during the first 6 months of measurements at Bogota. The statistics have been separated into two regions called west (west of the 74°W meridian) and east to longitudes eastward of this meridian.

substantial differences in scintillation activity at regions separated by few hundred kilometers. However, they have been observed to operate during magnetically disturbed times and are nearly absent during quiet or moderate conditions. Other ionospheric effects such as a longitudinal variation in the altitude of the *F* layer or a limited spatial extension of the prereversal enhancement seem unlikely to occur on a regular basis. Instead, we suggest that the source of the longitudinal variability resides in the different behavior of the gravity wave activity at regions separated by few degrees in longitude. *Meriwether et al.* [1996, 1997] have presented solar maximum observations of elevated thermospheric temperatures in the directions over the Andes, suggesting that gravity wave energy from the surface penetrates into the thermosphere, where viscous dissipation causes the heating. In addition, there exists a general consensus that gravity waves of mesospheric origin initiate the development of the equatorial plasma bubbles acting as a "seed" of the RTI mechanism [*Kelley et al.*, 1981]. On the basis of these arguments, we suggest that a higher population of gravity waves may exist over the Andes and the Amazon forest regions, enhancing the production of plasma bubbles in a region situated to the east of the 74°W meridian.

[14] **Acknowledgments.** The authors would like to thank M. Bevis and E. Kendrick of the University of Hawaii for providing the RINEX files from their Iquique, Copiapo, and Antuco stations; these stations are part of the South Andes Project (SAP). We thank M. P. Hagan for careful reading of the revised manuscript. We greatly appreciate the support of G. Bishop of the Air Force Research Laboratory and A. J. Mazzella of the Northwest Research Associates for allowing us to use the SCORE program. We thank Jorge Espinoza for providing the logistic support for the installation of receivers at Iquitos, Cuzco, and Pucallpa, and Ruben Villafani for their dedication to the smooth operation of several instruments at Ancon. The work at Boston College was partially supported by NSF grants ATM-9819912 and ATM-0123560, by Air Force Research Laboratory contract F19628-02-C-0087, and AFOSR task 2311AS. The observatory of Ancon is operated by the Geophysical Institute of Peru, Ministry of Education.

References

Basu, S., et al. (2001), Ionospheric effects of major magnetic storms during the international space weather period of September and October 1999: GPS observations, VHF/UHF scintillations and in situ density structures at middle and equatorial latitudes, *J. Geophys. Res.*, *106*, 30,389.

Devasia, C. V., N. Jyoti, K. S. V. Subbarao, K. S. Viswanathan, D. Tiwari, and R. Sridharan (2002), On the plausible linkage of thermospheric meridional winds with the equatorial spread *F*, *J. Atmos. Sol. Terr. Phys.*, *64*, 111.

Fejer, B. G., L. Scherliess, and E. R. de Paula (1999), Effects of the vertical plasma drift velocity on the generation and evolution of equatorial spread *F*, *J. Geophys. Res.*, *104*, 19,859.

Hysell, D. L., and J. D. Burcham (1998), JULIA radar studies of equatorial spread *F*, *J. Geophys. Res.*, *103*, 29,155.

Kelley, M. C., M. F. Larsen, C. A. LaHoz, and J. P. McClure (1981), Gravity wave initiation of equatorial spread *F*, *J. Geophys. Res.*, *86*, 9087.

Maruyama, T. (1988), A diagnostic model for equatorial spread *F*: 1. Model description and application to electric field and neutral wind effects, *J. Geophys. Res.*, *93*, 14,611.

Maruyama, T., and N. Matuura (1984), Longitudinal variability of annual changes in activity of equatorial spread *F* and plasma bubbles, *J. Geophys. Res.*, *89*, 10,903.

Mendillo, M., J. Baumgardner, X. Pi, P. J. Sultan, and R. Tsunoda (1992), Onset conditions for equatorial spread *F*, *J. Geophys. Res.*, *97*, 13,865.

Mendillo, M., J. Meriwether, and M. Biondi (2001), Testing the thermospheric neutral wind suppression mechanism for day-to-day variability of equatorial spread *F*, *J. Geophys. Res.*, *106*, 3655.

Meriwether, J. W., J. L. Mirick, M. A. Biondi, F. A. Herrero, and C. G. Fesen (1996), Evidence for orographic wave heating of the equatorial thermosphere at solar maximum, *Geophys. Res. Lett.*, *23*, 2177.

Meriwether, J. W., M. A. Biondi, F. A. Herrero, C. G. Fesen, and D. C. Hallenback (1997), Optical interferometric studies of the nighttime equatorial thermosphere: Enhanced temperatures and zonal wind gradients, *J. Geophys. Res.*, *102*, 20,041.

Valladares, C. E., W. B. Hanson, J. P. McClure, and B. L. Cragin (1983), Bottomside sinusoidal irregularities in the equatorial *F* region, *J. Geophys. Res.*, *88*, 8025.

Valladares, C. E., S. Basu, K. Groves, M. P. Hagan, D. Hysell, A. J. Mazzella Jr., and R. E. Sheehan (2001), Measurement of the latitudinal distributions of total electron content during equatorial spread *F* events, *J. Geophys. Res.*, *106*, 29,133.

Woodman, R. F., and C. LaHoz (1976), Radar observations of *F* region equatorial irregularities, *J. Geophys. Res.*, *81*, 5447.

R. E. Sheehan and C. E. Valladares, Institute for Scientific Research, Boston College, 140 Commonwealth Ave., Chestnut Hill, MA 02647, USA. (valladar@bc.edu)

J. Villalobos, Department of Physics, Universidad Nacional de Colombia, Bogota, Colombia. (ionosfera2001@yahoo.com)